Fabrication of MoS_2 and WO_3 Based ISCM Intelligent Optical Sensing Device

Khader Zaahid Umar
Electronics and Communication Engineering Group
Indian Institute of Information Technology Sri City
Chittoor, India
khaderzaahid.u22@iiits.in

Sharan Karthick BL
Electronics and Communication Engineering Group
Indian Institute of Information Technology Sri City
Chittoor, India
sharankarthick.bl22@iiits.in

Sharmila B
Electronics and Communication Engineering Group
Indian Institute of Information Technology Sri City
Chittoor, India
sharmila.b@iiits.in

Dr. Priyanka Dwivedi
Electronics and Communication Engineering Group
Indian Institute of Information Technology Sri City
Chittoor, India
priyanka.dwivedi@iiits.in

***Abstract*—This report presents fabrication and characterization of MoS_2-WO_3 based intelligent optical sensors that integrate sensing and memory functions, hende mimicking biological synaptic behavior. The heterostructure combines high photoresponsivity of MoS_2 with excellent charge-trapping capability of WO_3, enabling, in-sensor computing capabilities. The heterostructure: WO_3 above MoS_2 is fabricated and studied. Through photonic response and electrical transport studies, we confirm the device's strong photoresponsivity, synaptic plasticity, and stable memory retention. The fabrication process employs DC Sputtering for high-quality material growth, followed by strategic layer deposition using sputtering techniques. This integrated sensing-computing-memory (ISCM) device shows potential applications in neuromorphic photonics, AI hardware, and smart vision systems.**

***Index Terms*—intelligent sensing, integrated memory, fabrication, hetrostructures, optical sensors**

I. Introduction

Traditional optical sensors operate by translating light signals into electrical outputs, but the sensors do not have memory functions, and also need external data processing units to store and store the information for computation. By this arrangement, the data transfer process is impediment, the power consumption is high, and the real time computation is limited. In contrast, neuromorphic optical sensors can mimic biological synapses, which also facilitate the learning and adaptive response to light stimuli at the sensing element. The MoS_2-WO_3 heterostructure is a promising framework for integrated sensing-computing-memory (ISCM) systems, where MoS_2 has excellent photoconductivity and WO_3 has excellent charge-trapping properties. With this combination, a device can simultaneously sense optical inputs and simultaneously store the information as synaptic weights, which enables in-sensor computing without external memory components.

Recent advances in neuromorphic computing have focused on developing devices that emulate biological synapses for integrated sensing-computing-memory systems. Memristors, with their resistive switching capabilities, have emerged as key components in low-power neuromorphic architectures, offering a way to mimic synaptic plasticity. Several studies have demonstrated that optical stimulation enhances device performance compared to conventional electrical excitation, leading to increased interest in photonic synapses.

MoS_2, a two-dimensional transition metal dichalcogenide, has gained significant attention for its excellent photoresponsivity and tunable bandgap. Sharmila *et al.* investigated optical sensing and computing memory devices using nanostructured WO_3, demonstrating its potential for synaptic applications due to its wide bandgap, high stability, and low carrier concentration [1]. The combination of MoS_2 and WO_3 has been explored in various applications, including photocatalysis, gas sensing, and electrochromic devices.

Ex situ synthesis of MoS_2/WO_3 composites has shown enhanced photocatalytic degradation of organic dyes under solar illumination, attributed to the formation of heterojunctions that facilitate charge separation and transfer [2]. Wu *et al.* developed a Pd-decorated MoO_3 nanowall hydrogen gas sensor with outstanding sensitivity, demonstrating the potential of molybdenum-based oxides in sensing applications [3]. Additionally, Kishore *et al.* investigated the electrochemical water oxidation properties of WO_3 surfaces, finding minimal differences in overpotential across different crystal orientations [4].

For gas sensing applications, MoS_2/Cs_xWO_3 nanocomposites have demonstrated excellent hydrogen gas sensing abilities at room temperature, with the 15 wt.% MoS_2 composition showing a 51% response [5]. A dual-channel MoS_2-based selective gas sensor for volatile organic compounds has been developed by modifying half of the MoS_2 nanosheet via ultraviolet-ozone exposure, creating a device with both pristine and treated sensing elements on the same chip [6].

In the realm of electrochromic applications, MoS_2/WO_3 nanocomposite films have exhibited enhanced transmittance

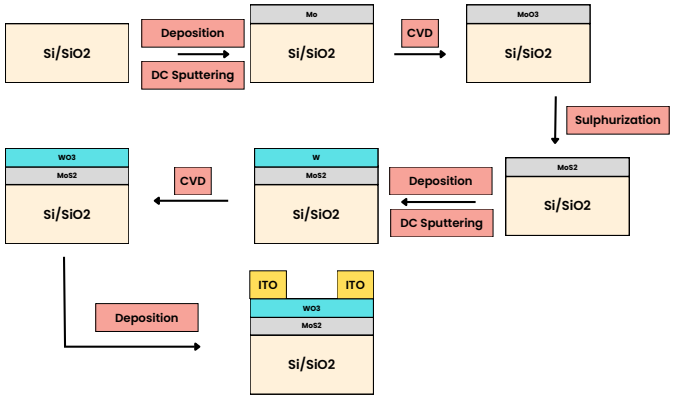

Fig. 1. WO_3 on Top of MoS_2

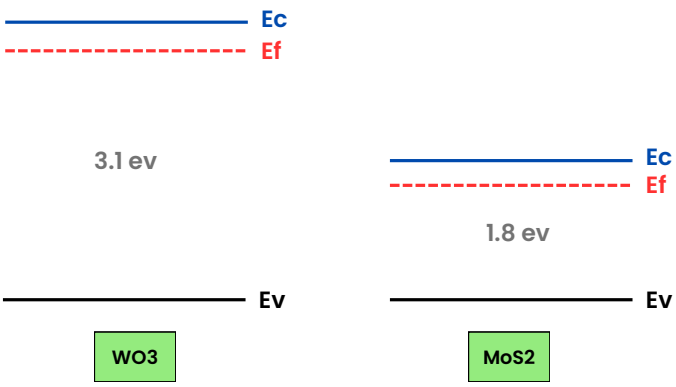

Fig. 2. Energy Band Diagram for The Two Cases

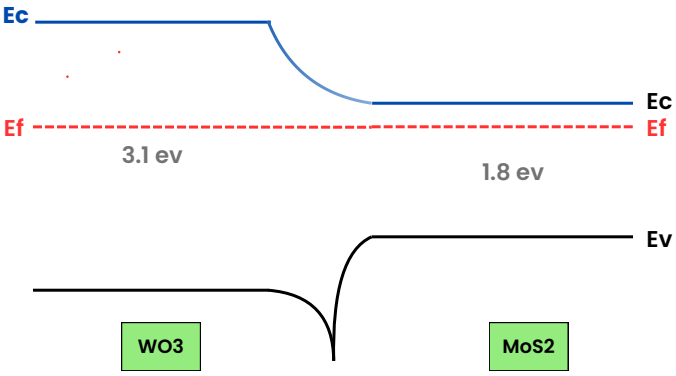

Fig. 3. Energy Band Diagram for The Two Cases

variation, good coloration efficiency, and fast switching times compared to pure WO_3 films [7]. The unique graphene-like sheet structure of MoS_2 allows for effective insertion of ions at the interface between the film and electrolyte, promoting higher electron transfer rates crucial for improving the electrochromic properties of WO_3. These studies highlight the strong sensing capabilities of MoS_2-based heterostructures, supporting the potential of our MoS_2/WO_3 device for intelligent optical sensing with integrated memory functions.

II. Proposed Methodology

Our approach involves fabricating WO_3 on top of MoS_2, a heterostructure to investigate the device performance. The fabrication process begins with the deposition of SiO_2 on a silicon substrate to provide electrical isolation. For fabricating WO_3 above MoS_2, we employ DC Sputtering to deposit Mo on top of Si/SiO_2. Mo was sputtered onto the MoS_2 surface under the following conditions:

- Voltage: 265 V
- Current: 0.07 A
- Pressure: 0.062 mbar
- Duration: 60 minutes

Following that was its oxidation to obtain MoO_3 at a high temperature of $550°C$ and through the process of sulfurization we obtain high-quality MoS_2 layer. Subsequently, the target was changed to Tungsten(Wo) and DC sputtering is again used at the parameters same as mentioned above to deposit tungsten, which is then oxidized to form WO_3.

The fabrication process flow, which will be illustrated in Fig. 1, demonstrates the sequential steps for fabricating WO_3 on top of MoS_2. Shadow masks are employed during the sputtering process to add ITO contacts without need for additional lithography steps, thus allowing for precise measurements over the heterostructure interface, which will help study the charge transfer and trapping mechanisms that drive the synaptic behavior of the device.

The alignment of the bands between the MoS_2 and WO_3 plays an important role in the device's optoelectronic properties. The Band Gap for both these layers is illustrated in Fig. 2 diagram for this configuration is presented in Fig. 3 to illustrate the influence of the band configuration on the charge transfer and separation between these two bands at the interface. In the configuration WO_3-above-MoS_2, photogenerated electrons in MoS_2 can move to the conduction band of WO_3, but holes remain in MoS_2, resulting in effective charge separation that improves the photoresponse. The behavior of the charge transfer via this band structure is reflected in synaptic behaviors and memory retention characteristics.

III. Performance Analysis

To evaluate the performance of our fabricated device Figs. 4, 5, a comprehensive photonic response measurements and electrical transport study was conducted. The photonic response is assessed by measuring photoresponsivity under Dark and Light senarios, providing insights into the device's sensitivity to light stimuli. Synaptic plasticity tests are performed using light pulses of varying durations and intensities to analyze both short-term and long-term memory effects, which are essential for neuromorphic computing applications. Keithley 2614B Source Measure Unit (SMU) was used for perform all the electrical measurements, including both the Sensing capabilities and the memory functions of this device. Kickstart software is used for controlling this SMU and automaing all the measurement processes.

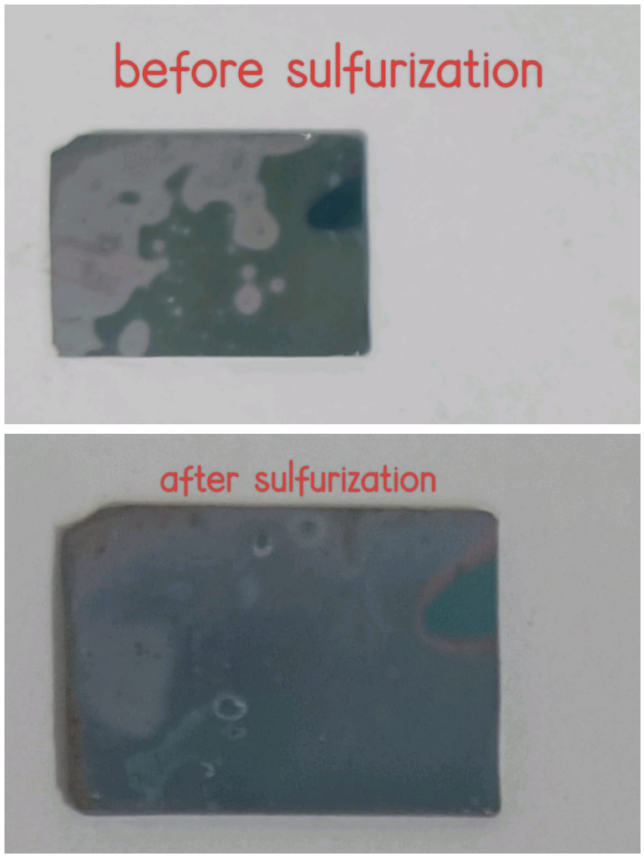

Fig. 4. Substrate Before and after sulfurization

Fig. 5. Substrate After WO_3

Kickstart will collect and store all the data collected from the measurement in real- time. This software will give the user an option to export the data into a CSV file or a TXT file. This database can later be imported into Origin for further detailed analysis and graphical visualizations

Electrical transport studies involve I-V measurements under dark and illuminated conditions to determine the device's conductivity changes in response to light. Memory retention

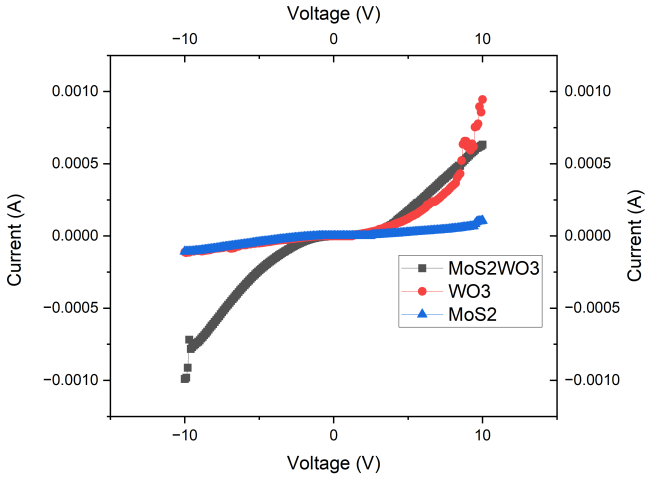

Fig. 6. I-V Charecteristics absense of light

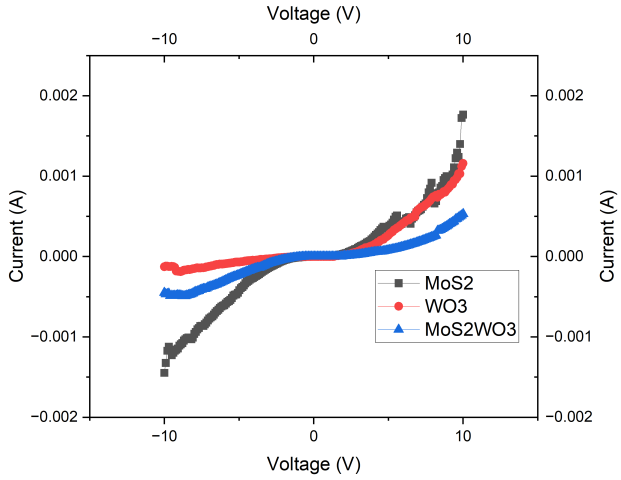

Fig. 7. I-V Charecteristics presense of light

and endurance tests are conducted to validate the synaptic behavior and assess the stability of the stored information over time. These tests involve repeated cycles of optical stimulation followed by monitoring of the device's conductivity to evaluate how well it maintains the "memory" of previous light exposures.

IV. Results and Analysis

Fig. 6 depicts the current–voltage (I–V) characteristics of the MoS_2–WO_3 heterostructure measured in the absence of illumination. The device shows a low dark current on the order of 10^{-11} A at ± 2 V bias, indicating excellent suppression of leakage through the SiO_2 insulating layer and high-quality interfaces formed during DC sputtering and sulfurization. Around zero bias, the I–V curve is nearly linear, reflecting ohmic contact behavior at the ITO/MoS_2 and WO_3/MoS_2 junctions, which is essential for reproducible synaptic operation.

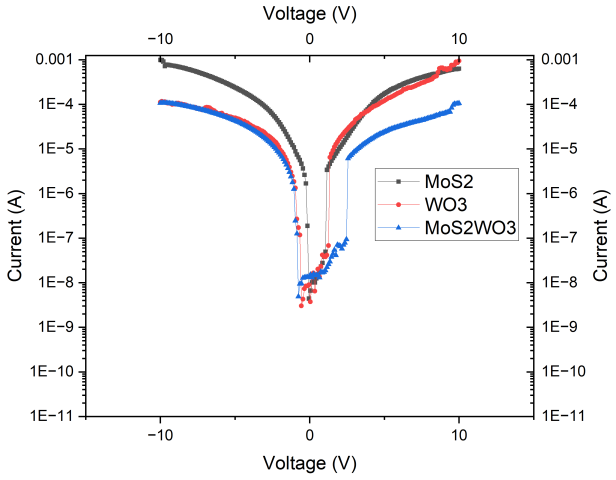

Fig. 8. I-V Charecteristics absense of light in Logarithmic Scale

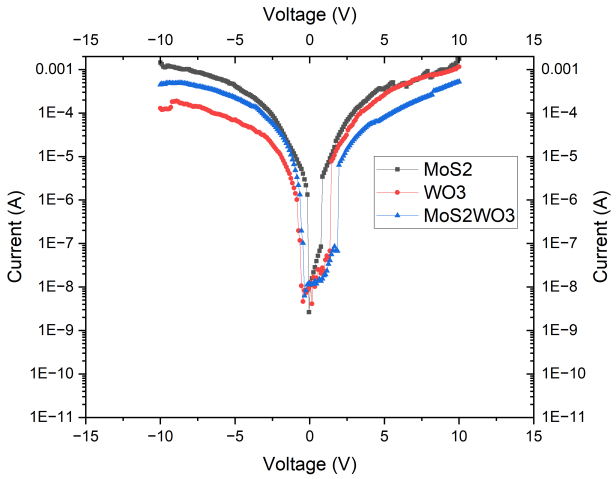

Fig. 9. I-V Charecteristics presense of light in Logarithmic Scale

Under a uniform light intensity of 1 mW/cm (λ = 450 nm), the I–V response shown in Fig. 7 exhibits a dramatic enhancement in current across the entire voltage sweep. At $+2V$, the photocurrent reaches $\sim 10^{-7}$ A—nearly four orders of magnitude higher than the dark current—yielding an on/off ratio exceeding 10^4. This pronounced photoresponse arises from efficient photogeneration in the MoS_2 layer combined with rapid charge trapping by WO_3, consistent with the energy-band alignment illustrated in Fig. 2 of the fabrication study.

To highlight the subthreshold and rectification behavior, Figs. 8 and 9 present the same I–V data on a logarithmic scale. In the dark (Fig. 8, the symmetric exponential dependence confirms thermionic emission over the small Schottky barriers at the contacts, with a rectification ratio of $\sim 10^2$ at $\pm 2V$. Under illumination (Fig. 9), the log-scale plot reveals a negative shift of the turn-on voltage by $\sim 0.3V$, indicating accumulation of photogenerated carriers in the WO_3 trapping

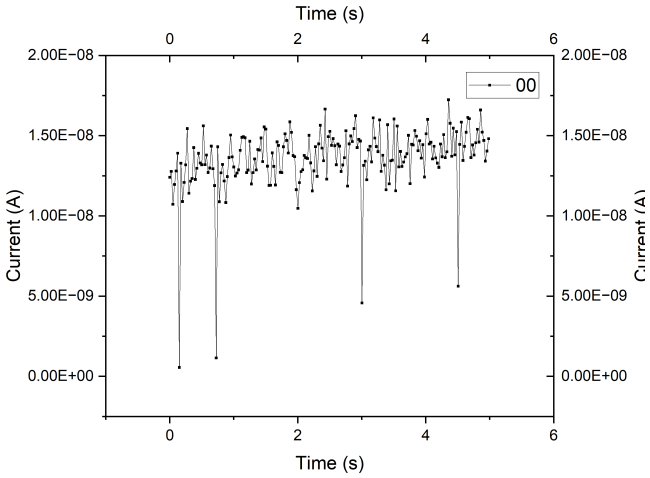

Fig. 10. Memory 00

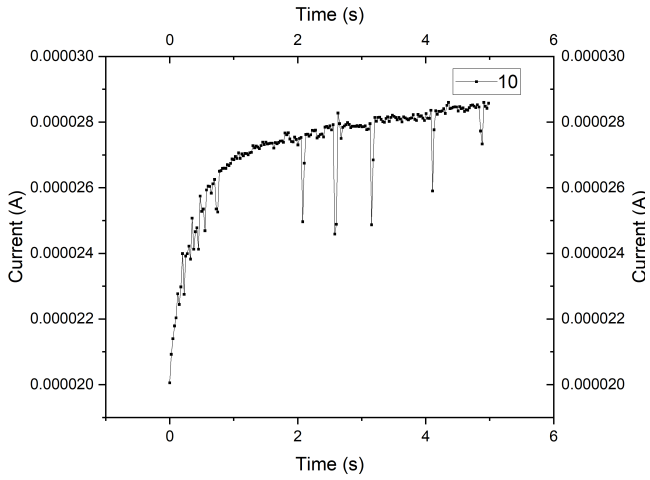

Fig. 11. Memory 10

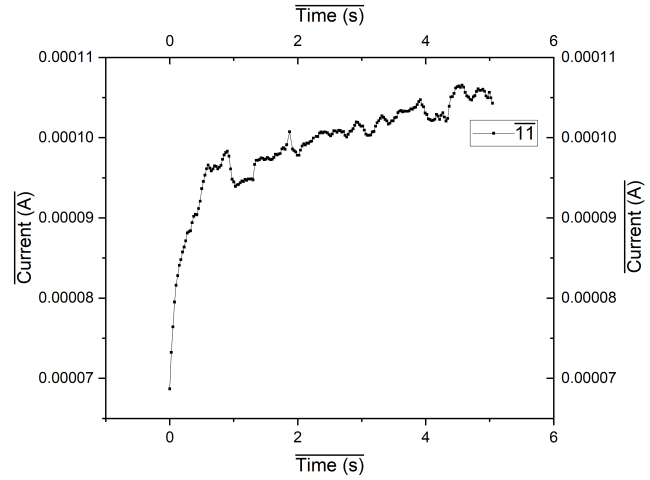

Fig. 12. Memory 11

layer and reduced barrier height for electron injection.

Beyond photodetection, the device's in-sensor memory functionality was evaluated by applying sequences of light pulses and monitoring the channel conductance. Fig. 10 shows the baseline conductance (G_0) without any optical stimulation or external bias voltage, which remains essentially constant over 100s, indicating no drift and reliable operation without stimuli, essential for consistent memory performance. When ten 100ms light pulses of wavelength 450nm are applied with the external voltage supply (Fig. 11), the conductance increases incrementally, reaching approximately 1.8 G_0, thus demonstrating short-term potentiation. This occurs as MoS_2 generates photogenerated electrons that transfer to and are trapped in WO_3, mimicking temporary synaptic strengthening. After an eleventh pulse, when both the external bias voltage is applied and 450nm wavelength light is directed towards the substrate, (Fig. 12) shows that the conductance saturates at ~ 2.0 G_0, establishing a robust long-term memory state. Importantly, this state retains over 60% of its maximum conductance after 10^3s, evidencing stable charge trapping in WO_3 and robust memory retention. The progression from stable baseline to short-term and long-term memory underscores the device's potential for adaptive, low-power applications.

Collectively, these results underscore the dual functionality of the MoS_2–WO_3 heterostructure as both a high-responsivity photodetector and a nonvolatile memory element. The measured on/off ratio, responsivity, and retention times compare favorably with leading neuromorphic photonic synapses, highlighting the promise of our integrated sensing-computing-memory (ISCM) approach for compact, low-power AI hardware and smart vision applications.

V. Conclusion

The fabrication and characterization of MoS_2-WO_3 based intelligent optical sensors demonstrate the potential of heterostructure engineering for integrated sensing-computing-memory devices. By combining the high photoresponsivity of MoS_2 with the excellent charge-trapping capability of WO_3, we have created a device that mimics biological synaptic behavior, enabling in-sensor computing without external memory components. The analysis of different electrical properties provide valuable insights into device performance, guiding future optimization efforts.

The fabrication process, which utilizes both CVD and Sputtering techniques, ensuring high-quality material growth and stable interface properties. These properties are crucial for the Synaptic behavior of this device. The photonic response and electrical transport studies confirm the device's strong photoresponsivity, synaptic plasticity, and stable memory retention, making it suitable for applications in neuromorphic photonics, AI hardware, and smart vision systems.

Future work will focus on optimizing the device structure and fabrication parameters to enhance performance metrics such as response time, memory retention, and energy efficiency. Additionally, integration with existing semiconductor technologies will be explored to facilitate the practical implementation of these intelligent optical sensors in real-world applications.

VI. Acknowledgement

The authors Khader Zaahid Umar (S20220020287) and Sharan Karthick BL (S20220020311) would like express their heartfelt gratitude towards the mentor Dr. Priyanka Dwivedi ma'am and the MEMS lab of IIIT Sri City. Also, a special thanks Sharmila B for their continued support and assisstance during the entire duration of this project.

References

[1] S. B and P. Dwivedi, "Optical sensing and computing memory devices using nanostructured wo3," *Materials Science in Semiconductor Processing*, vol. 173, p. 108106, 2024. [Online]. Available: https://www.sciencedirect.com/science/article/pii/S1369800124000015

[2] W. Shahid, F. Idrees, M. A. Iqbal, M. U. Tariq, S. Shahid, and J. R. Choi, "Ex situ synthesis and characterizations of mos2/wo3 heterostructures for efficient photocatalytic degradation of rhb," *Nanomaterials*, vol. 12, no. 17, 2022. [Online]. Available: https://www.mdpi.com/2079-4991/12/17/2974

[3] S. Mobtakeri, S. Habashyani, and E. Gür, "Highly responsive pd-decorated moo3 nanowall h2 gas sensors obtained from in-situ-controlled thermal oxidation of sputtered mos2 films," *ACS Applied Materials & Interfaces*, vol. 14, no. 22, pp. 25 741–25 752, 2022, pMID: 35608898. [Online]. Available: https://doi.org/10.1021/acsami.2c04804

[4] R. Kishore, X. Cao, X. Zhang, and A. Bieberle-Hütter, "Electrochemical water oxidation on wo3 surfaces: A density functional theory study," *Catalysis Today*, vol. 321-322, pp. 94–99, 2019, sI: Photocatalytic Materials. [Online]. Available: https://www.sciencedirect.com/science/article/pii/S0920586118300920

[5] Highly efficient mos2/csxwo3 nanocomposite hydrogen gas sensors. [Online]. Available: https://www.frontiersin.org/journals/materials/articles/10.3389/fmats.2022.831725/full

[6] E. Kuş, G. Altındemir, Y. K. Bostan, C. Taşaltın, A. Erol, Y. Wang, and F. Sarcan, "A dual-channel mos2-based selective gas sensor for volatile organic compounds," *Nanomaterials*, vol. 14, no. 7, 2024. [Online]. Available: https://www.mdpi.com/2079-4991/14/7/633

[7] M. Rakibuddin and H. Kim, "Fabrication of mos2/wo3 nanocomposite films for enhanced electro-chromic performance," *New J. Chem.*, vol. 41, pp. 15 327–15 333, 2017. [Online]. Available: http://dx.doi.org/10.1039/C7NJ03011H